Heat Transfer Characteristic Study of Solar Collector integrated with/without Phase Change Material (RT42)

Nhel Bundarith, Sarawut Polvongsri*

School of Renewable Energy, Maejo University

Abstract

This research aims to investigate the heat transfer phenomenon of a solar collector integrated with a phase change material (PCM). The various experiments are tested in different riser sizes, including a 16 mm tube (PCM1), a 10 mm tube (PCM2) that filled with PCM RT42, and a riser tube without PCM (conventional solar collector). These case studies are tested with different mass flow rates of 0.01, 0.02, and 0.03 kg/s•m^2, respectively, following ASHRAE 93-2003 standard condition used to analyze the collector system's thermal performance and heat transfer characteristics. Using PCM, the solar collector heat gains investigation reveals that the input temperature is adjusted low, resulting in significant energy absorption and minimal heat loss. The standard condition tested is setting the input temperature slightly higher, which revealed that the heat gain of the solar collector decreased while the heat loss increased under the limit ambient temperature. Both solar collectors with PCM (PCM1 and PCM2) are given the thermal performance represented by $F_R(\tau\alpha)_{e,}$ and F_RU_L gets higher than the conventional collector (without PCM). The highest thermal performance was achieved at a mass flow rate of 0.03 kg/s•m^2, following the same pattern as the changing convective heat transfer coefficient. The maximum convective heat transfer coefficient value is 131.06 W/m2•K of PCM1 while followed by PCM2 and without PCM, respectively. In addition, the empirical correlation equation for predicting the convective heat transfer coefficient of solar collectors integrated with PCM was presented.

Keywords: Solar Collector, Heat Transfer Characteristic, Phase Change Material

* *Corresponding author : sarawut-energy@hotmail.com*

Received: 11 เม.ย. 64; Revised: 8 ก.ค. 64; Accepted: 6 ต.ค. 64

1. Introduction

Nowadays, the world's energy demand is continuously increasing, especially for fossil fuels such as oil, coal, natural gas that emits a large amount of gas into the atmosphere and contributes to the greenhouse effect, air pollution, and climate change. Currently, renewable energies such as biomass, biofuel, wind energy, hydropower, and solar energy (IEA 2019) are widely known as green energies that reduce carbon emissions. One of the most popular renewable energy is solar energy; it is free, clean, and abundant on every continent. Solar energy can be converted into electricity and thermal energy, which can be used to power buildings and industries. Many types of collectors are used to create thermal energy for hot water, with the flat plate solar collector being one of them. It is command equipment that converts thermal energy from solar radiation into heat by circulating water from the collector to the storage tank, at temperatures ranging from 40 to 70^{o}C (Gautam et al. 2017; Sharples & Charlesworth 1998). However, many researchers were interested in upgrading systems to increase the water temperature in the solar water heating systems (SWHS). As an active solar water heating system, the integrated technique of solar collector performance enhancement is to boost the convection heat transfer coefficient by force water circulation in the system. The active SWHS was employed in several experiments, and it showed a higher performance than passive SWHS. Even though the heat transfer enhancement is a particular case that many researchers investigate in this field of study, new methods are constantly being developed to find an alternative way to integrate on flat plate solar collector and working fluid, such as using nano-particle, twist-tap, phase change materials and reflex surface for increasing time operation and absorbed heat ability. Although employing nano-particles as the working fluid of solar collectors can improve heat transmission and thermal performance during operation (Muhammad et al. 2016; Polvingsri & Kiatsiriroat 2014; Sharafeldin & Gróf 2018; Sharafeldin et al. 2017), it is still limited in use because the sediment reduces efficiency.

Phase Change Material (PCM) is a chemical composite with a high specific heat capacity for storing a large amount of thermal energy during the melting or freezing process. It is a popular thermal energy reservoir that can reduce heat loss, gives a suitable outlet temperature during a cloudy day, and can extend operating time compared to those without PCM (Gond et al. 2012; Gupta et al. 2017; Khalifa & Abdul Jabbar 2010; Khalifa et al. 2013; Wu et al. 2018). The case of PCM that fills in the solar collector does not improve the heat transfer between a collector and a working fluid because the thermal conductivity of PCM is very low; however, it can maintain

the fluid temperature higher than the ambient temperature after the solar collector operation is complete. Lin et al. (Lin et al. 2012) studied the flat plate collector integrated phase change material that extended surface into the PCM reservoir to increase the heat transfer area and operating time, while the result showed that the 120 liters of storage tank generated with mass flow rate at 0.5 kg/min produce hot water at 38^{o}C and daily efficiency of 52%. Papadimistatos et al. (2016) studied the integrating dual phase change material inside the evacuated tube solar collector. Their study immersed a heat pipe into the phase change material at 72^{o}C and 118^{o}C of melting temperature. The result showed that the system's heat released was delayed and could provide hot water during high using hours. Also, the efficiency improvement is 26% of normal operation and 66 % for the stagnation mode. Yang et al. (Yang et al. 2018) investigated the performance of PV/T with PCM and without PCM. The result showed that the heat stored in PCM could be discharged to the working fluid when the solar radiation is insufficient. Under a controlled indoor environment with solar radiation of 800 W/m^{2} and a water flow rate of 0.15 m^{3}/h, the primary energy-saving efficiency for the PV/T-PCM system would be increased by 14%. These results indicated that the integration of a PCM inside a PV/T system could improve the system's energy performance.

The thermosyphon flat plate collector consists of the twist-tap, wire, coil, and ring wire inserted into the collector absorber tube to increase the turbulent flow and heat transfer (Eiamsa-ard & Seemawute 2012; Jaisankar et al. 2009; Kalogirou 2014; Murugan et al. 2019). Both twist-tap and wire coil inserted into the collector absorber tube could improve the thermal efficiency because their surfaces were attached to the absorber collector, and the turbulent flow could transfer plenty of the working fluid. Balaji et al. (Balaji et al. 2018) studied a thermosyphon with rod and tube enhancers that were frictionally engaged with the inner tube side of the tube absorber wall for heat transfer augmenting and axial flow control. The result found that when pumping power increased minimally, the rod velocity enhancer provided a heat transfer rate higher than the tube velocity enhancer configuration. When compared to the plain tube, the increasing efficiency of rod and tube velocity enhancers were 15% and 10%, respectively. Saravannan et al. (2016) investigated the V-trough thermosyphon solar water heater with helically twisted tapes at various twist ratios (Y = 3, 4, 5, and 6) and compared it to the conventional solar water heater. The result showed that the helix twisted tape offered a significant enhancement of heat transfer, friction factor, and thermal efficiency compared to the plain V-trough collector. Especially, the helix twisted tape with minimum twist ratio 3 yielding

the maximum heat transfer enhancement compared with twist ratio 4, 5, 6, and PVT collector was 12.06%, 18.44%, 24.75%, and 60.84%, respectively. The twist ratio of helix twisted tape was reduced, which increased the friction factor. Garcia et al. (García et al. 2013) studied the heat transfer enhancement of a flat plate solar collector with wire-coil inserts. The result showed that the wire-coil could increase the average thermal efficiency in the range of 14-31% and the useful power collected with no additional pressure losses of up from 8 to 12% at the values of mass flow rates from 0.011 to 0.047 kg/s.

Sandhu et al. (2014) studied the related effects of inclination angle and insert devices on the flat plate solar collector with conventional and novel insertion configurations such as twisted-tape, wire coil, and wire mesh insertion. The result showed that all inserted devices could enhance Nusselt number, where the enhancement was apparent in transition and turbulent flow regimes while using the insertion of the concentric coils gave the best performance. The twisted-tape insert with the smallest pitch ratio performed the best insertion in the twisted-tape group. The recommend conclusion should choose a concentric coil which was enhancement Nusselt number 110% and gave a low Reynolds number.

Further, the conventional solar flat-plate collector had an average thermal efficiency of up to 70% from previous research using several techniques such as twist-plate and wire-coil with difference ratios inserted into the absorber plate of a collector. The thermal performance and convective heat transfer of the flat-plate solar collector with PCM incorporated could be affected when using the energy storage of PCM filled in the riser welded with baffle plate inserted into an absorber plate. Therefore, this study proposes to study the heat transfer enhancement of the solar collector with PCM inserted into the baffle plate riser tube with RT42 phase change material into absorber tube plate and comparing with a conventional solar collector under the same environmental conditions at the School of Renewable Energy, Maejo University, Chiang Mai, Thailand. The behavior of heat transfer will be discussed, as well as the heat transfer relationship.

2. Methodology

Solar collector with PCM

The conventional collector and solar collector integrated with PCMs are built in a single copper tube as an absorber plate tube with 28.7 mm of outside diameter, 1 mm of thickness, and 1,000 mm of length. For the solar collector with PCM, RT42 phase change material (PCM) with a melting point of 38 to 42^{o}C (ICNQT 2018) was inserted inside the riser copper tube with

different diameters of 10 mm and 16 mm. The riser tube surface was welded with ten baffle plates for water control. The configuration of the solar collector with PCM is shown in Figure 1 and Figure 2.

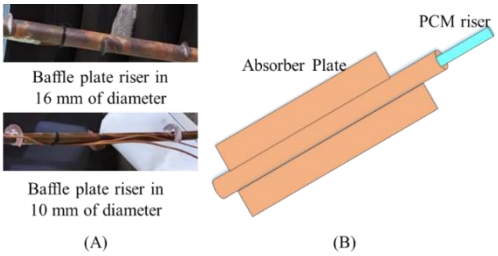

Figure 1 PCM riser tube (A) Baffle plate on the PCM riser tube surface, (B) PCM riser tube inserted into the absorber plate of a solar collector with PCM

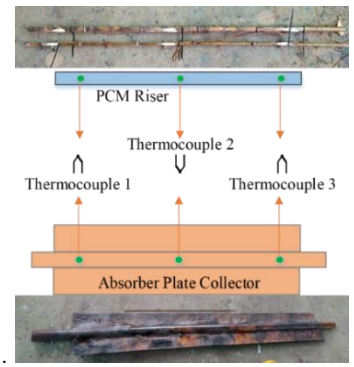

Figure 2 The absorber plate tube with 28.7 mm diameter and the PCM riser tube

The absorber plate surface was painted black for solar radiation absorption during the day. On top, a clear glass of 3 mm thickness was installed as a cover of the solar collector. All components are installed into a box covered with an aluminum frame and enfolded by the rubber insulation at the bottom and edge. The final dimension of the solar collector with PCM is 1,090 mm in length, 220 mm in width, and 100 mm in height, as shown in Figure 3. The characteristic of the solar collectors with PCM with different diameters of PCM riser tube is given in Table 2, including the conventional solar collector without PCM.

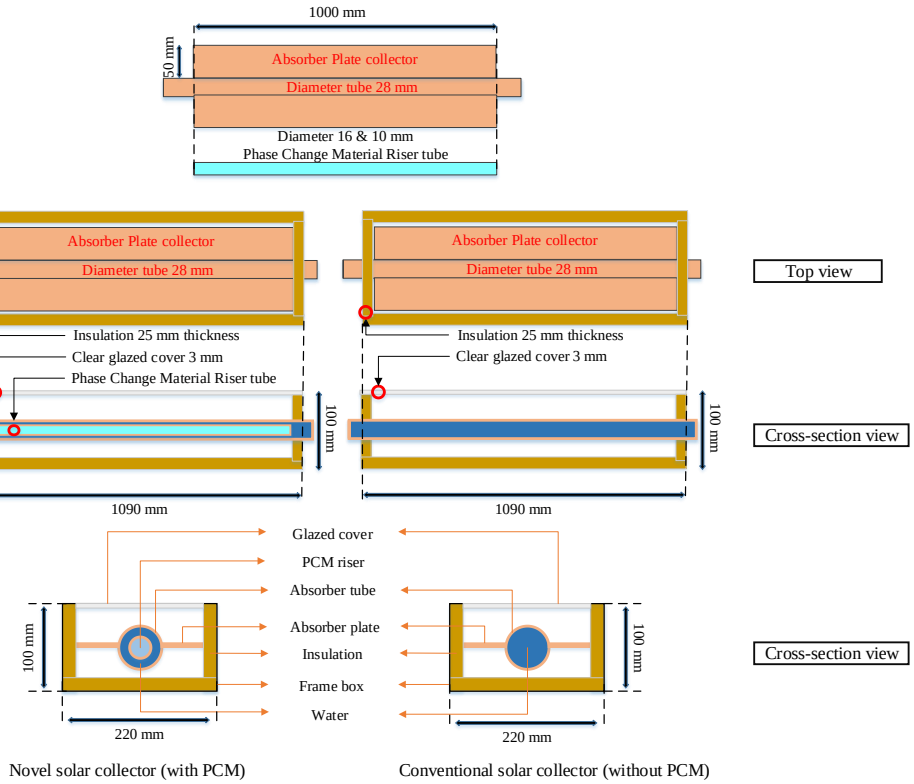

Figure 3 Schematic of the solar collector with PCM and conventional solar collector without PCM (A) Top view, (B) section view

Table 1 Physical properties and mass of the paraffin wax (ICNQT 2018).

RT42	Properties
Melting range	38-43°C
Heat storage capacity ±7.5%	165 KJ/kg
Specific heat capacity	3.5 kJ/(kg•K) Solid
	2.5 kJ/(kg•K) Liquid
Density solid at 15 °C	0.88 kg/l
Density liquid at 25 °C	0.77 kg/l
Heat conductivity (Both phases)	0.2 W/(m•K)
Volume expansion	12.5 %
Max. Operation temperature	72 °C

Table 2 The characteristic of solar collector PCM1, PCM2, and without PCM.

Category	Diameter	Unit	Inside
PCM 1	Ø 16	mm	RT 42
PCM 2	Ø 10	mm	RT 42
Without PCM	-	-	-

3. Experimental

The experiments were performed under the outdoor condition at the School of Renewable Energy, Maejo University, Chiang Mai, Thailand, located at a latitude of 18°N. The conventional and solar collectors with PCM were installed at 18° of tilt angle facing to the south. Each collector used the electric pump for water circulation from a storage tank through each solar collector. Inside the storage tank, the electric heater was installed for water temperature controlling during testing. The schematic of the experimental setup is shown in Figure 4 and Figure 5.

The solar collector integrated and conventional were tested following the ASHRAE Standard 93-2003 (Polvongsri 2013), which is shown in Table 3. The experiments were carried out at water temperatures ranging from 35 to 65°C. The temperature was set to increase by 5 °C, and data were recorded every 5 minutes in a multi-channel data logger.

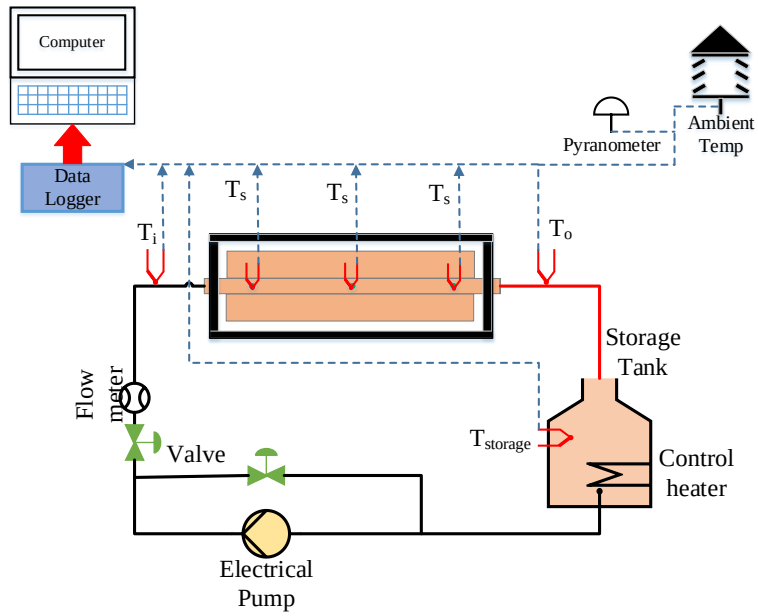

Figure 4 The schematic of the experimental setup

Figure 5 Solar collectors with PCM (PCM1, PCM2) and conventional solar collectors (without PCM) under outdoor testing

Table 3 ASHRAE 93-2003 standard condition of outdoor testing (Polvongsri 2013)

Variable	Maximum variation		Lower limit	Upper limit
	In between data periods	Within data periods		
Total irradiation normal to the sun	-	±32 W/m^2 (± 10 Btu/ft^2·h)	790 W/m^2	-
Fraction of diffuse radiation	-	-	-	20%
Incident angle modifier	-	±2%	-	-
Ambient Temperature	-	± 1.5°C	-	-
Wind speed	-	-	2.2 m/s	4.5 m/s
Flow rate	0.02 kg/s.m^2	± 0.005 gpm	-	-
Inlet Temperature	-	± Max of (1 °C, 2%)	-	-
Incident angle	-	± 2.5°	-	-
Symmetry to solar noon	-	-	-	-
Solar collector area	0.128 m^2			

Because the ASHRAE 93-2003 standard specifies a standard mass flow rate of 0.02 kg/s•m^2, the range of mass flow rate used in this study was selected below and upper values of the standard mass flow rate of 0.01, 0.02, and 0.03 kg/s•m^2, respectively. The mass flow rate in the system was measured by a flow meter (Model: Platon, accuracy ± 1.25%). The gauge valve was used to adjust the water flow and has a bypass valve for overload to prevent overpressure. The thermocouple type K (temperature range -270 to 1,260°C, ±0.4%) was used to measure all temperature points and recorded in a multi-channel data logger (Model: TD-1947 SD, accuracy ± (0.4%+0.5°C) and Model: Adam, accuracy ±0.2%). The solar radiation was measured using a pyranometer (Model: Apogee SP-110-L-10, Mul.5.0, accuracy ±5%).

4. Theory

The convective heat transfer coefficient inside the absorber tube of the solar collector can be calculated using the following Equation (1).

$$h_i = \frac{q''}{T_T - T_w} \tag{1}$$

Where q'' is the actual heat flux that can be calculated from the heat gain using the solar collector (Q_{coll}) and the collector area A_c by equation (2).

$$q'' = \frac{Q_{coll}}{A_i} \tag{2}$$

The heat gain from the solar collector Q_{coll} was calculated using the following equation (3).

$$Q_{coll} = \dot{m} C_p (T_o - T_i) \tag{3}$$

The heat gain from the novel solar collector integrated with phase change material was calculated using the following equation (4):

$$Q_{coll+PCM} = \dot{m} C_p (T_o - T_i) + \left(\mathrm{MC_p}\right)_{PCM} \left(\frac{dT}{dt}\right) \tag{4}$$

The enthalpy of PCM was calculated using equation (5) (ICNQT 2018):

$$h = \begin{cases} C_{ps}\left(T - T_{ref}\right), T < T_m \\ C_{ps}\left(T_{ms} - T_{ref}\right) + \dfrac{T - T_{ms}}{T_{ml} - T_{ms}} l, T_{ms} < T < T_{ml} \\ C_{ps}\left(T_{ms} - T_{ref}\right) + l + C_{pl}\left(T - T_{ml}\right), T > T_{ml} \end{cases} \tag{5}$$

The Reynolds number is a dimensionless ratio of the flow regime that depends mainly on the ratio of inertia force to viscous force in the fluid. It was expressed for the internal flow of circular pipe or duct using the following equation (6).

$$\mathrm{Re} = \frac{4\dot{m}}{\mu\pi D} \quad (6)$$

The convection heat transfer coefficient of water in the solar collector (h_i) was calculated using equation (7).

$$h_i = \frac{N_u k}{L} \quad (7)$$

The characteristics of water changed following the temperature variation; therefore, the properties of water were calculated using the mean temperature of water (T_w) (Balaji, et al. 2017). The mean temperature of the water is given by equation (8).

$$T_w = \frac{T_o + T_i}{2} \quad (8)$$

The specific heat of water that changed following the temperature circulating in the solar collector was calculated using equation (9).

$$C_p = 4226 - 3.244T_w + 0.0575T_w^2 - 0.0002565T_w^3 \quad (9)$$

The density of water that changed following the temperature circulating in the solar collector was calculated using equation (10).

$$\rho = 1001 - 0.08832T_w - 0.003417T_w^2 \quad (10)$$

The thermal conductivity of water that changed following the temperature circulating in the solar collector was calculated using equation (11).

$$k = 0.557 + 0.002198T_w - 0.00000708T_w^2 \quad (11)$$

The quality kinematic viscosity of water changed following the temperature circulating in the solar collector was calculated using equation (12).

$$\nu = \left[\left(\frac{1}{0.515 + 0.0119T_w}\right) - 0.12\right]10^{-6} \quad (12)$$

The thermal efficiency of the solar collector is defined as the ratio between the heat gain from the solar collector versus the total heat from incident solar radiation on the absorber plate (Duffie and Beckman 2013; Polvongsri 2013) using the following equation (13).

$$\eta = \frac{Q_{coll}}{I_T A_C} \quad (13)$$

The thermal efficiency is presented at near-normal incidence conditions so that F_R is constant of maximum efficiency and FR and UL are constant within the temperature range. The

linear equation emerges when the efficiencies are calculated using averaged data and plotted against (Ti-Ta)/IT (14).

$$\eta = F_R(\tau\alpha)_e - F_R U_L \frac{(T_o - T_i)}{I_T} \quad (14)$$

5. Results and Discussion

The results of the experiment at different mass flow rate of 0.01, 0.02 and 0.03 kg/s.m^2 are discussed in terms of the difference of outlet and inlet temperature, heat loss (U_L), heat removal factor (F_R), heat gain from the solar collector (Q_{coll}), thermal performance, and convective heat transfer coefficient (H_i).

Figure 6 presents the temperature difference between the outlet and inlet temperature (T_o-T_i) from solar collector PCM1, PCM2, and without PCM at various mass flow rates. The temperature difference of PCM1 is highest, followed by PCM2 and without PCM, respectively. The temperature difference of PCM1 and PCM2 is in a range of 10.1 to 4.22^{o}C and 9.22 to 4.1^{o}C at mass flow rate 0.01 kg/s▪m^2, 6.1 to 2.9^{o}C and 5.5 to 2.22^{o}C at mass flow rate 0.02 kg/s▪m^2 and 4.92 to 2.4^{o}C and 4.1 to 2.0^{o}C at the mass flow rate 0.03 kg/s▪m^2. While without PCM gives the temperature difference of 8.4 to 4.1^{o}C, 5.5 to 2.2^{o}C, and 4.1 to 2.4^{o}C following the various inlet temperatures.

When considering the water mass flow rate that affects the water temperature difference (To-Ti), it was found that the water temperature increased because water could receive more heat from solar radiation at the low mass flow rate. Considering the solar collector heat loss (U_L) in Figure 7, it was found that when the inlet water temperature increases and the water flow rate decreases, the U_L increases in all cases. The mass flow rate of 0.01 kg/s▪m^2 has the highest U_L, followed by 0.02 and 0.03 kg/s▪m^2, respectively. This phenomenon describes how water can absorb more solar heat at low mass flow rates than at high flow rates, causing the water temperature to rise. Furthermore, because the temperature differential between the water in the solar collector and the ambient temperature is so large, more heat is transmitted to the environment. Therefore, the U_L at low mass flow rates is higher than those at high flow rates.

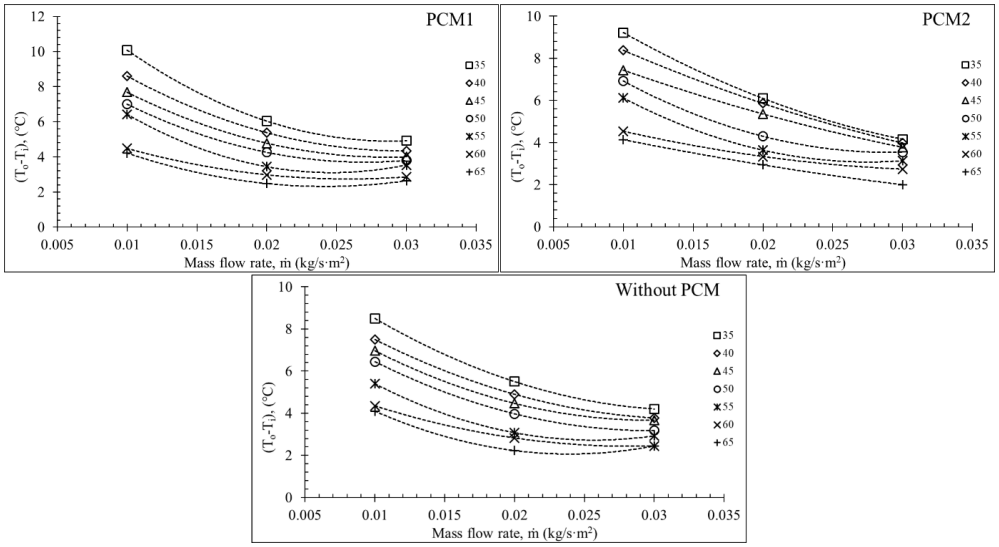

Figure 6 The temperature difference (T_o-T_i) of solar collector PCM1, PCM2, and without PCM at the mass flow rates of 0.01, 0.02, and 0.03 kg/s▪m^2.

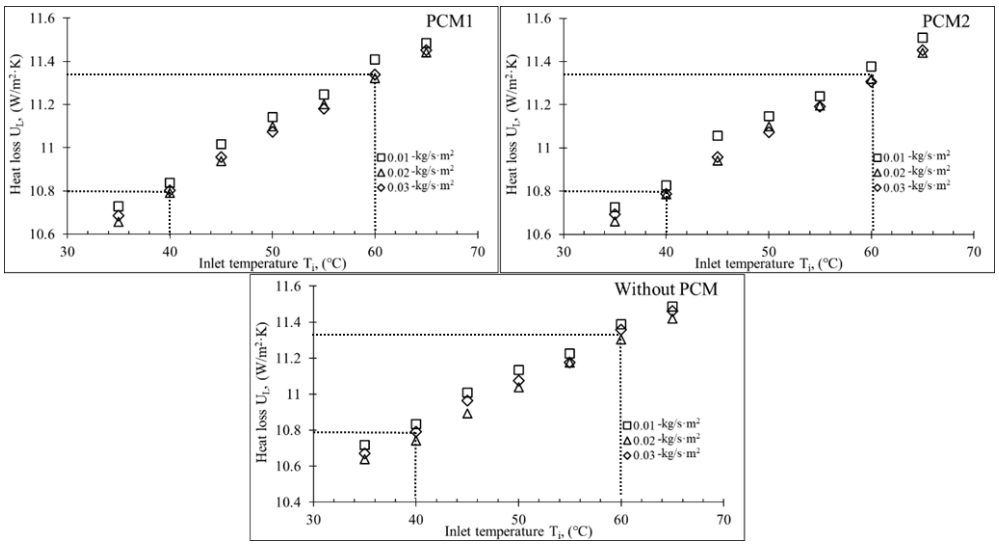

Figure 7 The heat loss (U_L) of solar collector PCM1, PCM2, and without PCM at the mass flow rates of 0.01, 0.02, and 0.03 kg/s▪m^2.

Figure 8 shows the heat removal factor (FR) variation at various mass flow rates and inlet temperatures. The results reveal that if the solar collector integrated with the PCM riser tube operates at a low mass flow rate, the low heat removal factor is reversed, while a high mass flow rate results in a high heat removal factor. From the calculations, the heat removal

factor of PCM1 and PCM2 from 35 °C to 65 °C are 0.78 to 0.65 and 0.78 to 0.63 at 0.01 kg/s▪m^2, 0.84 to 0.77 and 0.81 to 0.67 at mass flow rate 0.02 kg/s▪m^2. While the heat removal factor of 0.03 kg/s▪m^2 from 35 °C to 65 °C is 0.84 to 0.75 and 0.83 to 0.71, respectively. For the conventional solar collector (without PCM), the heat removal factor is 0.78 to 0.58, 0.81 to 0.60 and 0.83 to 0.63 at 0.01, 0.02, and 0.03 kg/s▪m^2, respectively. From the graph, PCM1 at a mass flow rate of 0.02 kg/s▪m^2, it was found that the heat removal factor increased with higher energy absorbed by working fluid in the system greater, while the amount of the fluid through the system is medium.

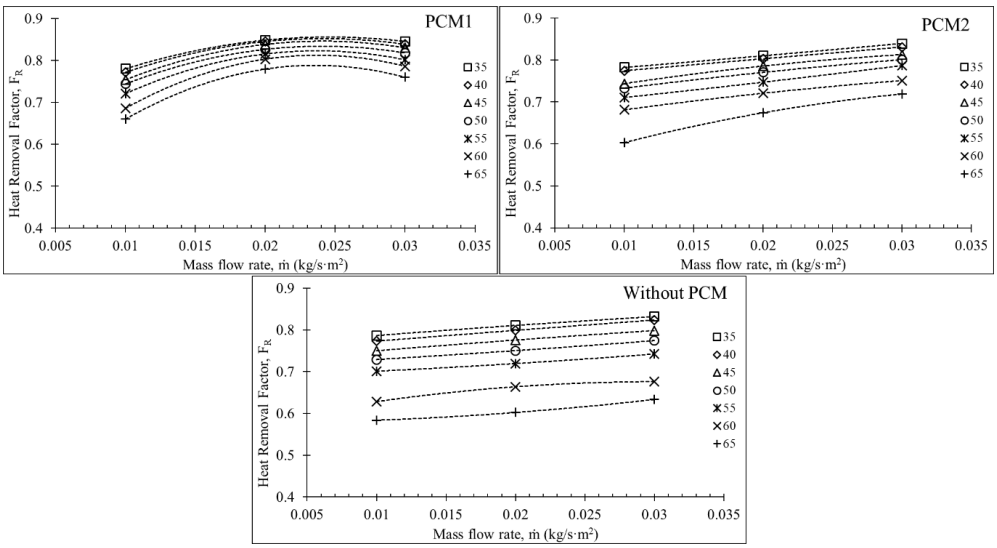

Figure 8 The heat removal factor (F_R) of solar collector PCM1, PCM2, and without PCM at the mass flow rates of 0.01, 0.02, and 0.03 kg/s▪m^2

The heat gained from solar collectors is shown in Figure 9. When the water was circulated at a low inlet temperature, the solar collector absorbed a significant amount of thermal energy; however, when the water was circulated at a high inlet temperature, the collectors with PCM only collected a small amount of thermal energy during testing. In addition, the mass flow rate influences the heat gain ($Q_{coll+PCM}$) of solar collectors with PCM; at all mass flow rates, heat gain obtained from solar collectors with PCM is higher than those without PCM. Where heat gain of PCM1 at the mass flow rate of 0.03 kg/s is a maximum value of 79.0 - 44.85 W, heat gain decreased when the inlet temperature was increased. For discussion of PCM2, the heat gain is maximum at the flow rate of 0.02 kg/s within a range of 68.2-32.92 W. Finally, in

the case of without PCM, the heat gain at the flow rate of 0.03 kg/s is maximum with 66.5-39.3 W. From the graph of PCM2, it was shown that the energy collected by solar collector integrated with riser 10 mm phase change material has a high energy change at a mass flow rate of 0.02 kg/s•m^2. Also, for different temperatures with mass flow rate tests at 65, 60, 55, 45, and 45 ^{o}C, it was found that the energy at mass flow rate 0.02 kg/s•m^2 was lower than that at mass flow rate 0.03 kg/s•m^2.

The thermal efficiency of conventional and solar collectors with PCM was measured using the linear regression analysis following the ASHRAE 93-2003 standard. When $F_R(\tau\alpha)_e$. on the Y-axis was plotted against $(T_i-T_a)/I_T$ on the X-axis, the slope of the linear line represented the heat loss (F_RU_L). Figure 10 shows the thermal efficiency of conventional and solar collectors with PCM with various mass flow at 0.01 kg/s•m^2, 0.02, kg/s•m^{2,} and 0.03 kg/s•m^2. Due to the enormous amount of PCM receiving the most heat from solar radiation, it was discovered that every mass flow rate of PCM1 delivers the highest thermal efficiency, followed by PCM2 and without PCM, respectively. Taking $F_R(\tau\alpha)_e$ and F_RU_L into account, it was found that at a mass flow rate of 0.03 kg/s, PCM1 had the highest thermal performance with $F_R(\tau\alpha)_e$ of 0.8354 and F_RU_L 9.6808 W/m^2•K, followed by PCM2 and without PCM with values of 0.7429, 8.7643 W/m^2•K and 0.7024, 8.6955 W/m^2•K, respectively.

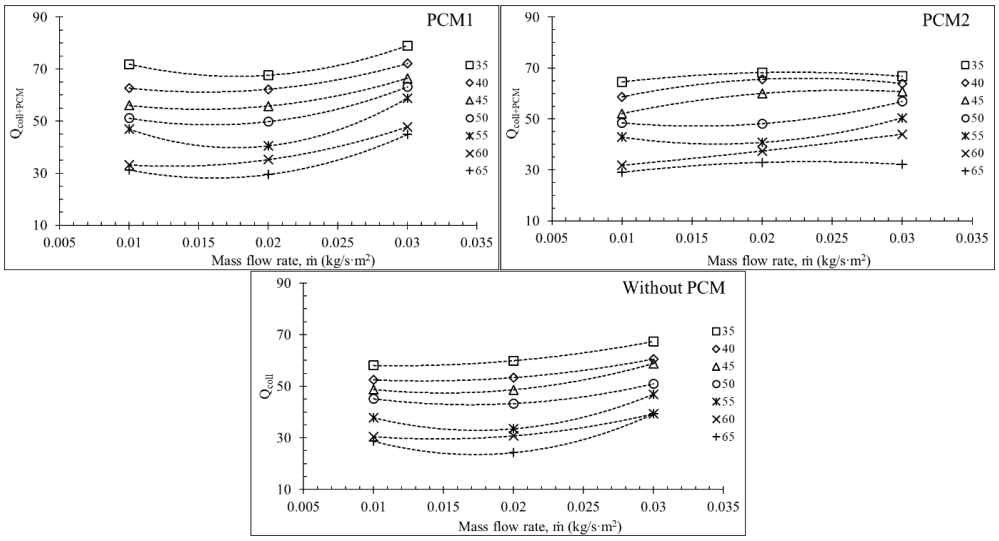

Figure 9 The heat gain of solar collector PCM1, PCM2, and without PCM at the mass flow rates of 0.01, 0.02, and 0.03 kg/s•m^2

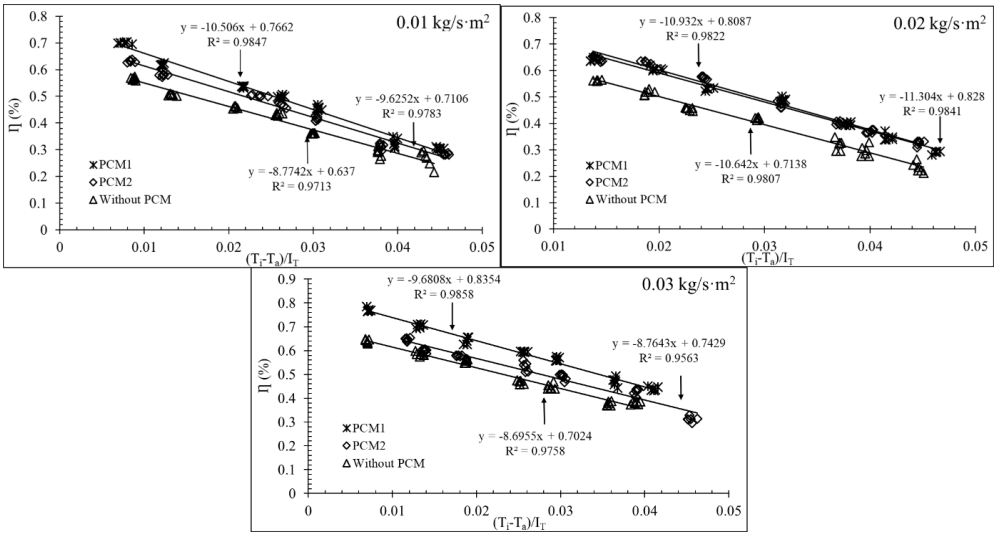

Figure 10 Thermal performance of solar collector PCM1, PCM2, and without PCM at the mass flow rates of 0.01, 0.02, and 0.03 kg/s▪m^2

Figure 11 presents the convective heat transfer coefficient (h_i) at various mass flow rates and inlet temperatures. All cases studied showed that h_i increased when mass flow rate increased; however, the convective heat transfer coefficient h_i decreased when the inlet temperature increased. This was due to the PCM riser inserted into the absorber plate. The 16 mm of PCM1 riser has a more inner surface that influences heat absorption of fluid, so PCM had high heat gain. While the PCM2 has a smaller PCM riser tube than PCM1, it had minimal effects on heat absorption. The convective heat transfer coefficient of PCM1 and PCM2 from 35°C to 65°C are 134.2 to 52.2 W/m^2▪K and 127.34 to 36.5 W/m^2▪K at mass flow rate of 0.01 kg/s▪m^2, 142.8 to 72.1 W/m^2▪K and 136.3 to 49.1 W/m^2▪K at mass flow rate of 0.02 kg/s▪m^2, and 157.9 to 75.3 W/m^2▪K and 139.8 to 56.1 W/m^2▪K at mass flow rate of 0.03 kg/s▪m^2, respectively. The convective heat transfer coefficient for the conventional solar collector without PCM is 122.5 to 32.06 W/m^2▪K, 131.06 to 32.8 W/m^2▪K, and 128.1 to 35.2 W/m^2▪K following the inlet temperature from 35°C to 65°C, respectively.

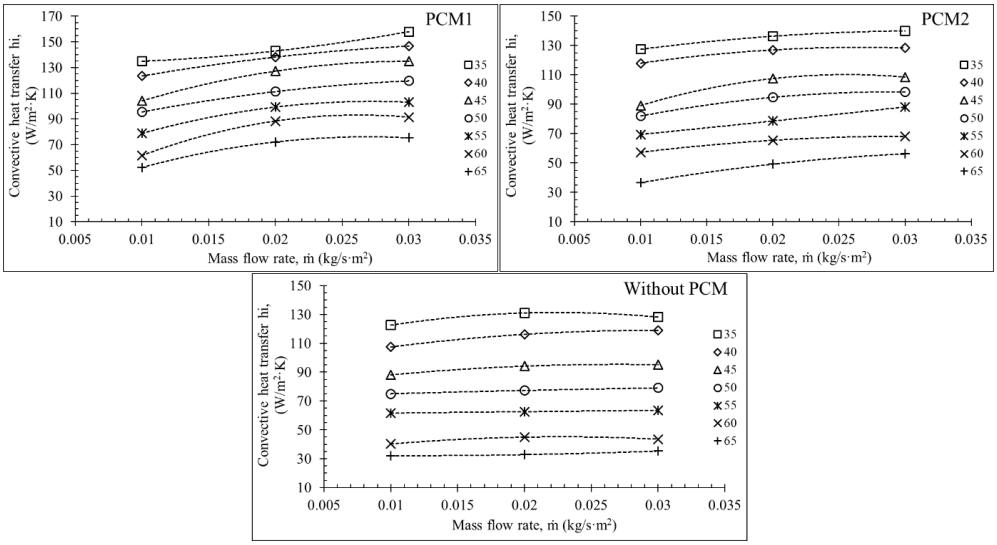

Figure 11 The convective heat transfer coefficient (h_i) of solar collector PCM1, PCM2, and without PCM at the mass flow rates of 0.01, 0.02, and 0.03 kg/s▪m^2

Figure 12 shows the variation of Nusselt Number (Nu) and Reynold Number (Re) of solar collectors with PCM at various mass flow rates and inlet temperatures. The Reynold Number (Re) of PCM1 is higher than that of PCM2, indicating a high-velocity inner flow of the absorber plate changed in a range 250 to 880 of PCM1, 170 to 590 of PCM2, and 110 to 380 of the conventional solar collector (without PCM), respectively. Prandtl number (Pr) was affected in a range of 4.51 to 2.7 of inlet temperature between 35 °C to 65 °C. The relation between the convective heat transfer coefficient in the absorber plate to working fluid (water) was presented as Nusselt Number (Nu). It was found that the Nu of PCM1 and PCM2 are 5.98 to 2.11 and 5.76 to 1.55 at a mass flow rate of 0.01 kg/s▪m^2, 6.5 to 2.9 and 6.2 to 2.1 at a mass flow rate of 0.02 kg/s▪m^2, and 7.16 to 3.1 and 6.34 to 2.4 at a mass flow rate of 0.03 kg/s▪m^2, respectively. The Nu of the solar collectors without PCM is 5.4 to 1.37, 6.1 to 1.41, and 6.13 to 1.5, following the inlet temperature from 35 °C to 65 °C, respectively. From the experiment, the solar collectors PCM1 and PCM2 are determined by the correlation of Nusselt number, Reynold number, and Prandtl number as:

Correlation: $$Nu = 0.143\,\mathrm{Re}^{0.19}\,\mathrm{Pr}^{1.821}$$

Where Prandtl number is 2 < Pr < 5. The relationship of Nusselt number (Nu) between the calculations and the experiment is presented in Figure 13.

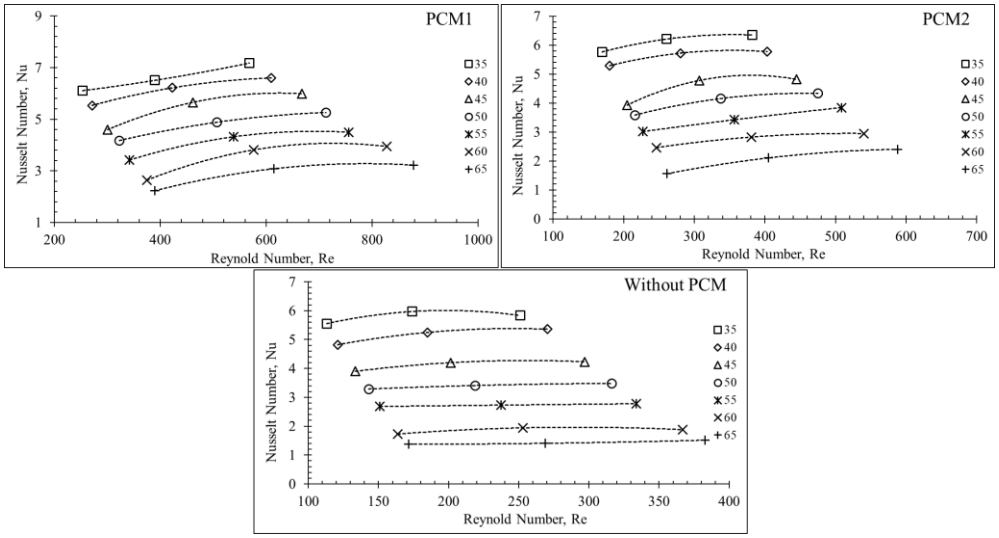

Figure 12 The Nusselt Number (N_u) of solar collector PCM1, PCM2, and without PCM

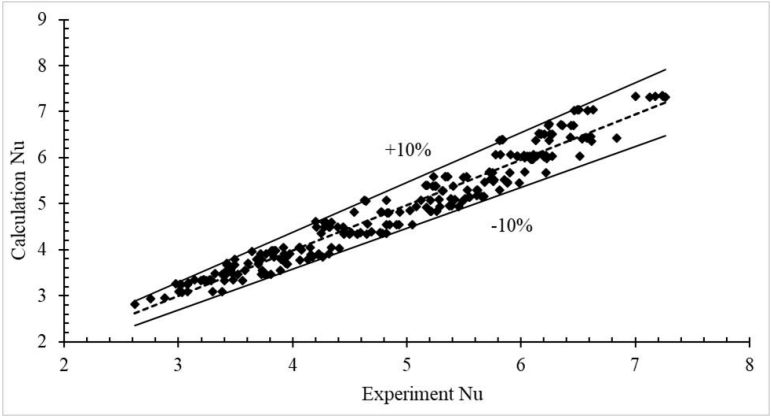

Figure 13 The relationship of Nusselt number (Nu) between calculation and experiment.

6. Conclusions

The solar collectors with PCM are built from a 28.7 mm diameter single tube integrated with phase change material in different diameters of 16 mm and 10 mm of the riser tube. Each riser is welded with ten small baffle plates for water flow direction controlling and increasing the collector's heat receiving capacity. The RT42, a selected type of Phase change material, is filled in the riser tube, and the solar collector is tested following ASHRAE standard 93-2003 at various mass flow rates of 0.01, 0.02, and 0.03 kg/s▪m^2 and inlet temperature from 35 to 65^{o}C. When the mass flow rate is high and the inlet temperature is low, the heat gain from solar collectors with PCM is high, whereas when the mass flow rate is low and the inlet temperature

is low, the temperature differential (T_o-T_i) is high. The convective heat transfer coefficient (h_i) from solar collector integrated with PCM (PCM1 and PCM2) is higher than the conventional solar collector (without PCM) by about 20%. Additionally, the correlation of heat transfer dimensionless is represented as $Nu = 0.143\,\mathrm{Re}^{0.19}\,\mathrm{Pr}^{1.821}$ with a relative error percentage of about 10%.

7. Acknowledgements

The authors would like to express their gratitude to the School of Renewable Energy, Maejo University, for supporting the study with a grant under the program, Strategic Scholarships from “Project and Development of the Renewable Energy Potential Graduates ASEAN”. We would like to thank the Smart Energy and Environmental Research Unit (SEEU) staff for supporting us with lots of suggestions, knowledge, and instruments.

8. References

Balaji, K., Iniyan, S., & Goic R. (2018). Thermal performance of solar water heater using velocity enhancer. *Renewable Energy, 115,* 887-895. https://doi.org/10.1016/j.renene.2017.09.014

Balaji, K., Iniyan, S., & Muthusamyswami, V. (2017). Experimental investigation on heat transfer and pumping power of forced circulation flat plate solar collector using heat transfer enhancer in absorber tube. *Applied Thermal Engineering*, *112*, 237-247. https://doi.org/10.1016/j.applthermaleng.2016.09.074

Duffie, John A., and William A. Beckman. (2013). *Solar engineering of thermal processes*. New Jersey: Wiley.

Eiamsa-ard, S., & Seemawute. P. (2012). Decaying swirl flow in round tubes with short-length twisted tapes. *International Communications in Heat and Mass Transfer, 39*(5), 649-656. https://doi.org/10.1016/j.icheatmasstransfer.2012.03.021

García, A., Martin, R. H., & Pérez-García, J. (2013). Experimental study of heat transfer enhancement in a flat-plate solar water collector with wire-coil inserts. *Applied Thermal Engineering*, *61*(2), 461-468. https://doi.org/10.1016/j.applthermaleng.2013.07.048

Gautam, A., Chamoli , S., Kumar, A., & Singh, S. (2017). A review on technical improvements, economic feasibility and world scenario of solar water heating system. *Renewable and Sustainable Energy Reviews, 68*(1), 541-562. https://doi.org/10.1016/j.rser.2016.09.104

Gond, B. K., Gaur, M. K., & and Malvi, C. S. (2012). Manufacturing and performance analysis of solar flat plate collector with phase change material. *International Journal of Emerging Technology and Advanced Engineering*, *2*(3), 456-459. https://ijetae.com/files/Volume2Issue3/ IJETAE_0312_78.pdf

Malvi, C. S., Gupta, A., Gaur, M. K., Crook, R., & Dixon-Hardy, D. W. (2017). Experimental investigation of heat removal factor in solar flat plate collector for various flow configurations. International Journal of Green Energy, *14*(4), 442-448. https://doi.org/10.1080/15435075.2016.1268619

Jaisankar, S., Radhakrishnan, T. K., & Sheeba, K. N. (2009). Experimental studies on heat transfer and friction factor characteristics of thermosyphon solar water heater system fitted with spacer at the trailing edge of twisted tapes. *Applied Thermal Engineering*, *29*(5), 1224-1231. http://www.rericjournal.ait.ac.th/index.php/reric/article/download/486/303

Kalogirou, S. A. (2014). Flat-plate collector construction and system configuration to optimize the thermosiphonic effect. R*enewable Energy, 67,* 202-206. https://doi.org/10.1016/j.renene.2013.11.021

Khalifa, A. J. N., & Jabbar, R. A. A. (2010). Conventional versus storage domestic solar hot water systems: A comparative performance study. *Energy Conversion and Management, 51*(2), 265-270. https://doi.org/10.1016/j.enconman.2009.09.021

Khalifa, A. J. N., Suffer, K. H., & Mahmoud, M. Sh. (2013). A storage domestic solar hot water system with a back layer of phase change material. *Experimental Thermal and Fluid Science, 44,* 174-181. https://doi.org/10.1016/j.expthermflusci.2012.05.017

Lin, S. C., Al-Kayiem, H. H., & Aris, M. S. B. (2012). Experimental investigation on the performance enhancement of integrated PCM-flat plate solar collector. *Journal of Applied Sciences, 12*(24), 2390-2396. https://doi.org/10.3923/jas.2012.2390.2396

Muhammad M. J., Mahmud S. A., Sidik, N. A. C., Yazid, M. N. A. W. M., Mamat, R., & Najafi, G. (2016). The use of nanofluids for enhancing the thermal performance of stationary solar collectors: A review. *Renewable and Sustainable Energy Reviews, 63*, 226-236. https://doi.org/10.1016/j.rser.2016.05.063

Murugan, M., Vijayan, R., Saravanan, A., & Jaisankar, S. (2019). Performance enhancement of centrally finned twist inserted solar collector using corrugated booster reflectors. *Energy, 168*, 858-869. https://doi.org/10.1016/j.energy.2018.11.134

Papadimitratos, A., Sobhansarbandi, S., Pozdin, V., Zachidov, A., & Hassanipour, F. (2016). Evacuated tube solar collectors integrated with phase change materials. *Solar Energy, 129*, 10-19. https://doi.org/10.1016/j.solener.2015.12.040

Polvingsri, S., & Kiatsiriroat, T.(2014). Performance analysis of flat-plate solar collector having silver nanofluid as a working fluid. *Heat Transfer Engineering, 35*(13), 1183-1191. https://doi.org/10.1080/01457632.2013.870003

Polvongsri, S. (2013). Ashrae Standard 93-2003 Methods of testing to determine the thermal performance of flat-plate solar Collectors. School of Renewable Energy Maejo University. 5-9.

Sandhu, G., Siddiqui, K., & Garcia, A. (2014). Experimental study on the combined effects of inclination angle and insert devices on the performance of a flat-plate solar collector. *International Journal of Heat and Mass Transfer, 71,* 251-263. https://doi.org/10.1016/j.ijheatmasstransfer.2013.12.004

Saravanan, A., Senthilkumaar, J. S., & Jaisankar, S. (2016). Experimental studies on heat transfer and friction factor characteristics of twist inserted V-trough thermosyphon solar water heating system. *Energy, 112,* 642-654. https://doi.org/10.1016/j.energy.2016.06.103

Sharafeldin, M. A., & Gróf, G. (2018). Experimental investigation of flat plate solar collector using CeO_2-water nanofluid. *Energy Conversion and Management, 155*, 32-41. https://doi.org/10.1016/j.enconman.2017.10.070

Sharafeldin, M. A., Gróf, G., & Mahian, O. (2017). Experimental study on the performance of a flat-plate collector using WO_3/Water nanofluids. *Energy, 141,* 2436-2444. https://doi.org/10.1016/j.energy.2017.11.068

Sharples, S., & Charlesworth, P. S. (1998). Full-scale measurements of wind-induced convective heat transfer from a roof-mounted flat plate solar collector. *Solar Energy, 62*(2), 69-77. https://doi.org/10.1016/S0038-092X(97)00119-9

Wu, W., Dai, S., Liu, Z., Dou, Y., Hua, J., Li, M., Wang X., & Wang X. (2018). Experimental study on the performance of a novel solar water heating system with and without PCM. *Solar Energy, 171*, 604-612. https://doi.org/10.1016/j.solener.2018.07.005

Yang, X., Sun, L., Yuan, Y., Zhao, X., & Cao, X. (2018). Experimental investigation on performance comparison of PV/T-PCM system and PV/T system. *Renewable Energy, 119*, 152-159. https://doi.org/10.1016/j.renene.2017.11.094